Selenium-containing compound ameliorates lipopolysaccharide-induced acute lung injury via regulating MAPKs/AP-1 pathway

Wenjing Jia (15067897058@163.com)

Department of Geriatric Medical, First Affiliated Hospital of Wenzhou Medical University;Chemical Biology Research Center, School of Pharmaceutical Sciences, Wenzhou Medical University

https://orcid.org/0000-0001-8938-9515

Wenting Ding

Chemical Biology Research Center, School of Pharmaceutical Sciences, Wenzhou Medical University

Xinmiao Chen

Chemical Biology Research Center, School of Pharmaceutical Sciences, Wenzhou Medical University

Zhengwei Xu

Chemical Biology Research Center, School of Pharmaceutical Sciences, Wenzhou Medical University

Yeilin Tang

Chemical Biology Research Center, School of Pharmaceutical Sciences,Wenzhou Medical University

Meihong Wang

Chemical Biology Research Center, School of Pharmaceutical Sciences, Wenzhou Medical University

Bin Zheng

Chemical Biology Research Center, School of Pharmaceutical Sciences, Wenzhou Medical University

Yali Zhang

Department of Geriatric Medical, First Affiliated Hospital of Wenzhou Medical University; Chemical Biology Research Center, School of Pharmaceutical Sciences, Wenzhou Medical University

Tao Wei

Chemical Biology Research Center, School of Pharmaceutical Sciences, Wenzhou Medical University

Zaisheng Zhu

Department of Geriatric Medicine,First Affiliated Hospital of Wenzhou Medical University

---

Research Article

Keywords: Acute lung injury, LPS, Inflammation, MAPK

Posted Date: April 7th, 2021

DOI: https://doi.org/10.21203/rs.3.rs-306616/v1

Version of Record: A version of this preprint was published at Inflammation on September 6th, 2021. See the published version at https://doi.org/10.1007/s10753-021-01521-z.

Abstract

Acute lung injury (ALI) characterized by a series of inflammatory reactions and served as the main cause of mortality in intensive care unit patients. Although great progress have been made in understanding the pathophysiology of ALI, there are no effective treatment in clinic. Recently, we have synthesized a selenium-containing compounds, which possess obvious anti-inflammatory activity. The aim of the present study is to evaluate the protective effects of the selenium-containing compound **34#** in LPS-induced ALI in mice as well as its underlying mechanism. Compound **34#** was found to inhibit LPS-induced macrophage inflammatory cytokine release. These effects were observed to be produced via suppression of the MAPKs/AP-1 pathway. Compound **34#** was also noted to attenuate the LPS-induced lung inflammation in mice with ALI. The corresponding results suggested that compound **34#** possesses remarkable protective effects on LPS-induced ALI. Furthermore, the MAPKs/AP-1 pathway may prove to be its the underlying mechanism. Accordingly, compound **34#** may serve as a potential candidate for the prevention of ALI.

Introduction

Acute lung injury (ALI) is characterized by acute diffuse lung injury due to various internal and external lung factors. ALI always follows a series of inflammatory reactions, such as increased pulmonary capillary permeability, release of inflammatory mediators, and pulmonary interstitial and alveolar edema. Diffuse alveolar injury increases pulmonary microvascular permeability, leading to pulmonary edema and hyaline membrane formation, which may also be accompanied by pulmonary interstitial fibrosis. ALI physiologically manifests as decreased lung volume, decreased lung compliance and severe ventilation/blood flow imbalance, which clinically manifests as acute and progressive hypoxic respiratory insufficiency. When ALI progresses further and shows signs of obvious respiratory distress, refractory hypoxemia or even respiratory failure, it is termed acute respiratory distress syndrome (ARDS)[1]. A previous study has demonstrated that among ICUs in 50 countries, the period prevalence of ARDS was 10.4% of ICU admissions, having a high mortality rate[2]. Current treatment methods and effects of ALI/ARDS are very limited. In addition to treating the primary disease, the main treatments are respiratory support treatment, fluid management and other supportive therapies[3]. Therefore, determining effective drugs for the treatment of ALI is of clinical significance.

Excessive inflammation is known to play an important role in ALI. Excessive inflammation includes the infiltration of inflammatory cells and release of cytokines, such as inflammatory factors, adhesion molecules and chemokines[4]. Lipopolysaccharide (LPS) is the main cell wall component of Gram-negative bacteria. LPS is commonly used to establish the ALI model, which explores the mechanism and potential therapies of ALI. There is growing evidence that LPS can activate MAPK pathways, such as c-Jun NH2-terminal kinase (JNK), extracellular signal-regulated kinase (ERK), and p38 pathways, which stimulates the production of various inflammatory factors, leading to lung tissue injury [5].

Selenium is an important trace element found in the human body. Selenium decrease was found to be correlated with many severe diseases. Manzanares et al. has reported that selenium decreased early in serum/plasma in critically ill patients suffering from sepsis/septic shock[6]. Selenium administration can diminish many diseases, such as apoptosis[7], cancers[8], diabetes[9], liver injury[10] and lung injury[11, 12]. Meanwhile, compounds containing selenium in their structure have demonstrated significant antifungal[13], anticancer[14, 15] and anti-inflammatory [16] activities. Recently, we have synthesized a selenium-containing compound 3-(phenylselanyl)-1H-pyrrolo[2,3-b]pyridine (**34#**, Fig. 1a). In this study, we illustrate its anti-inflammatory activities and its underlying mechanism in conjunction with its protective effects on LPS-induced ALI.

Materials And Methods

Reagents

Lipopolysaccharide (LPS) was obtained from Sigma-Aldrich (St.Louis, MO, USA). Antibodies for P38, p-P38, JNK, p-JNK, ERK, p-ERK, p-c-jun, c-jun, GAPDH, and IκB were obtained from Cell Signaling Technology (Danvers, MA, USA). Anti-F4/80 was purchased from Santa Cruz Biotechnology (Dallas, TX, USA). Anti-LY6G was obtained from Abcam (Cambridge, UK). Antibodies for CD11B, CD45 and LY6Cwere obtained from BD Pharmingen (New York, USA). The mouse TNF-α and IL-6 ELISA kits were purchased from eBioscience (San Diego, CA, USA). Compound **34#** was synthesized in our lab and structurally identified using MS and ^{1}H-NMR analyses. For *in vivo* studies, **34#** was dissolved in 0.5% carboxymethylcellulose sodium (CMCNa) in water solution and 0.5% CMCNa alone was used as vehicle control. For cell culture studies, **34#** was dissolved in dimethyl sulfoxide (DMSO), and the same volume of DMSO alone was used as the vehicle control.

Cell culture

Mouse primary peritoneal macrophage (MPMs) were prepared from male C57BL/6 mice. C57BL/6 mice were intraperitoneal (i.p.) injected of 2.5 mL starch broth which was constituted with 1 g tryptone, 0.5 g NaCl, 6 g soluble starch and 0.3 g beef extract, and boiled in 100 mL double-distilled H_2O. After 2 days, peritoneal macrophages were collected by washing the peritoneal cavity with 10 mL RPMI-1640 medium (Gibco, Eggenstein, Germany) per mouse. The cells were centrifuged and resuspended in RPMI-1640 medium with 10% fetal bovine serum (FBS) (Hyclone, Logan, UT, USA). The macrophages were cultured at 37 °C in 5% CO_2-humidified air. Four hours later, the non-adherent cells were removed by washing with PBS. Firmly adhered macrophages were used for experiments.

Animal care and ALI mouse model

Male C57BL/6 mice (18–20 g) were obtained from the Animal Centre of Wenzhou Medical University (Wenzhou, China). Animals were housed at a constant room temperature with a 12:12 h light-dark cycle and fed with a standard rodent diet for at least 7 days before used in the Animal Centre of Wenzhou Medical University. All animal care and experimental procedures were approved by the Wenzhou Medical

University Animal Policy and Welfare Committee (Approval Document No. wydw2019-0438). All animals received humane care according to the National Institutes of Health (USA) guidelines.

The C57BL/6 mice were randomly divided into four groups (n=8 per group). The groups consisted of vehicle control (CON), LPS-induced ALI group (LPS), **34#** treatment of LPS-induced ALI (LPS+**34#** 10 mg/kg), **34#** treatment-only group (**34#** 10 mg/kg). Mice were given 10 mg/kg/day **34#** for 3 continuous days by gavage, then challenged with intratracheal instillation of 5 mg/kg LPS or equal volume 0.9% saline. Mice were euthanized with chloral hydrate 6 h after LPS injection, lung tissues, broncho alveolar lavage fluid (BALF) and blood samples were collected.

MTT assay

MPMs were seeded into 96-well plates at a density of 5 x 10^4 cells per well in RPMI-1640 medium with 10% FBS, 100 U/mL penicillin and 100 mg/mL streptomycin. Cells were incubated with different concentrations of **34#** (2.5, 5, 10, 20 and 40 μM) for 24 h. Then, 20 μL MTT (5 mg/mL) was added to all wells, and the plate was incubated in 5% CO_2 at 37 °C for another 4 h. Cells were dissolved with 150 μL DMSO and were then analyzed in a multi-well-plate reader at 490 nm.

Determination of cytokines

After treatment of cells with **34#** and LPS, TNF-α and IL-6 content in culture medium and serum were determined by ELISA according to manufacturer's instructions (Bioscience, San Diego, CA). The total amount of TNF-α or IL-6 in medium was normalized to the protein concentration of lysates.

RNA extraction and Real-time quantitative PCR

MPMs and lung tissues (10-20 mg) were homogenized in TRIZOL (Invitrogen, Carlsbad, CA, USA) for total RNA extraction. The purity of the sample was estimated by calculating the OD ratio (A260/A280, ranging from 1.8 to 2.2). Both reverse transcription and Quantitative PCR (qPCR) was carried out using IQ SYBR Green Supermix (Bio-Rad, Hercules, CA, USA). QuantStudio®3 Real Time PCR Systems (ABI, CA, USA) was used for qPCR analysis. The primers of the target genes are listed in the Table 1 and were obtained from Invitrogen (Shanghai, China).

Western blot assay

MPMs were pretreated with DMSO (vehicle) or 10 μM **34#** for 30 min, which was followed by 0.5 μg/mL LPS for 15 min. Collected cells or homogenized lung tissues were then lysed. Concentration of total proteins was determined using the Bradford assay (Bio-Rad, Hercules, CA, USA).

Lysates were separated by sodium dodecyl sulfate-polyacrylamide gel electrophoresis and were electro-transferred to a nitrocellulose membrane. The membranes were then blocked for 1.5 h at room temperature in Tris-buffered saline (pH 7.6) containing 0.05% Tween 20 and 5% non-fat dry milk. Primary antibody incubations were carried out at 4 °C overnight. Secondary antibodies were then introduced for 1

h at room temperature. Immunoreactivity was visualized using enhanced chemiluminescence reagents (BI, Beit Haemek, Israel) and was quantified using Image J analysis software version 1.38e (NIH, Bethesda, MD, USA). Values were normalized to their respective protein controls.

BALF analysis

A tracheal cannula was inserted into the primary bronchus, and BALF was performed through the cannula using Ca^{2+} / Mg^{2+}-free PBS. Approximately 0.8 mL BALF was acquired. The collected BALF was centrifuged at 3000 rpm for 10 min at 4 °C. The supernatant was then immediately stored at -80 °C for protein concentration and cytokine determination. The sediment was resuspended in 50 μL physiological saline in order to determine the number of total cells using a cell counting instrument (Count star, Shanghai, China).

Flow cytometric analysis

The cells were resuspended in the collected BALF in PBS without Ca^{2+}/Mg^{2+}. The cells were mixed in the BALF of each group of mice together in pairs, after which 100 μL cell suspension was taken from each tube. Next, CD11B, CD45 and LY6C antibodies were used to stain the cells for 30 min. The cells were then washed with 1 mL PBS, centrifuged at 5000 rpm for 5 min, and resuspended with 500 μL PBS. ACCURI C6 PLUS (488 nm) flow cytometer and Flow Jo software were then used to analyze the cell subpopulations.

Histopathology and immunohistochemistry

Lung tissues were fixed in 4% paraformaldehyde, embedded in paraffin and sectioned at 5 μm thickness. After dehydration, sections were stained with hematoxylin and eosin (H&E) and were evaluated for general histopathological damage using light microscopy (Nikon, Japan).

Paraffin sections were also used to perform immunohistochemistry for CD68 and LY6G using routine techniques. Sections were then deparaffinized, rehydrated, treated with 3% H_2O_2 for 30 min to block endogenous peroxidase activity, and blocked with 1% BSA for 30 min. Slides were incubated overnight at 4 °C with primary antibodies, and immunoreactivity was detected by diaminobenzidine (DAB). Slides were counterstained with hematoxylin for 5 min, dehydrated, and mounted for viewing by bright field microscopy (Nikon, Japan). The percentage expression was measured using Image J software (NIH, Bethesda, MD, USA).

MPO

MPO test kit was used to measure myeloperoxidase (MPO) activity in lung tissue. The lung tissue was homogenized according to the kit's instructions, and was centrifuged at 12000 rpm at 4°C for 10 min. The supernatant was then taken for MPO activity detection and indicated in the form of U/g protein. BCA assay was used to determine the total protein content in the sample.

Statistical analysis

All experiments were randomized and blinded. *In vitro* experiments were repeated at least three times. All data are expressed as Mean ± SEM. All statistical analyses were performed using GraphPad Pro Prism 8.0 (GraphPad, San Diego, CA). We used one-way ANOVA, followed by Dunn's post hoc test when comparing multiple independent groups. Differences between group means were considered statistically significant at $p < 0.05$.

Results

Compound 34# inhibits LPS-induced expression of inflammatory cytokines in MPMs

In order to test the cytotoxicity of compound **34#**, the MTT assay was used. Fig. 1b illustrates that compound **34#** at 2.5, 5, 10, 20 and 40 μM did not show obvious cytotoxicity. The effects of compound **34#** on LPS-induced tumor necrosis factor-α (TNF-α) and interleukin-6 (IL-6) secretion were evaluated through an ELISA assay. Mouse peritoneal macrophages (MPMs) were pretreated with different concentrations (2.5, 5, 10, 20 and 40 μM) of **34#** for 30 min and were stimulated with LPS for 24 h. The corresponding results demonstrated that, compared to the blank control group, LPS significantly increased the production of TNF-α (Fig. 1c) and IL-6 (Fig. 1d). Moreover, the **34#** pretreatment dose-dependently inhibited LPS-induced inflammatory cytokine release.

Meanwhile, the gene expression of inflammatory mediators was detected by real time quantitative PCR (RT-qPCR). MPMs were pretreated with different concentrations (5, 10 and 20 μM) of **34#** for 30 min and were stimulated by LPS for 6 h. The results (Fig.1e and 1f) showed that LPS significantly increased the gene expression of inflammatory cytokines (TNF-α, IL-6, IL-1β), adhesion molecules (ICAM-1, VCAM-1) and chemokine (MCP-1). However, pretreatment with **34#** dose-dependently inhibited the LPS-induced increased.

Compound 34# inhibited LPS-induced MAPKs phosphorylation in MPMs

MAPKs/AP-1 and NF-κB signaling pathways are two typical down-stream pathways of LPS/TLR4. The effects of **34#** on LPS-stimulated MAPKs phosphorylation and NF-κB activation were further analyzed, which demonstrated that LPS significantly increased the phosphorylation of JNK, ERK and P38, which were obviously inhibited by **34#** treatment (Fig. 2a-c). The phosphorylation of c-jun, an AP-1 subunit, was found to be increased after LPS stimulation, whereas it was observed to be decreased by **34#** pretreatment (Fig. 2d). Unfortunately, compound **34#** had no effect on LPS-induced degradation of IκB-α and phosphorylation of P65 (Fig. 2e and f). The results indicated that the MAPKs/AP-1 signaling pathway may mediate the anti-inflammatory activity of **34#**, whereas NF-κB does not.

34# diminishes the severity of LPS-induced ALI in mice

Since **34#** has a significant effect on LPS-induced inflammation *in vitro*, its ability to protect against LPS-induced lung inflammation *in vivo* was examined, thus establishing an ALI model. First, the severity of lung injury was measured via H&E staining (Fig. 3a). Histological analyses demonstrated marked

inflammatory cell infiltration and alveolar wall thickening. In addition, LPS exposed mice were found to have vascular congestion in the lungs, which were dramatically reduced after pretreatment with **34#**. The lung injury scores (Fig. 3b) represent the degree of damage to lung tissues. The corresponding results suggested the protective effect of **34#** in LPS-induced lung injury. Moreover, the lung hyperpermeability marker, total protein concentration in BALF, exhibited the same results as that of H&E (Fig. 3c).

34# reduced LPS-induced inflammatory cell infiltration in lung tissue

The previous results suggested that LPS can induce lung hyperpermeability and infiltration of inflammatory cells. Here, the effect of **34#** was evaluated and showed that **34#** pretreatment can reduce total cell number in BALF, which was found to be induced by LPS (Fig. 4a). The number of neutrophils (Fig. 4b) in BALF was verified in regard to the effect of **34#** in relieving inflammatory cell infiltration. MPO is a marker of neutrophil activity. The corresponding results showed that the activity of MPO was reduced after treatment with **34#** (Fig. 4d). Furthermore, flow cytometry was used to detect the content of monocytes in BALF (Fig. 4c). The number of monocytes was found to be remarkably increased 6 h after LPS exposure, which was significantly reduced following **34#** administration. Moreover, immunohistochemical staining was performed in order to evaluate the recruitment of macrophages and neutrophils in lung tissues. Moreover, the macrophage marker CD68 (Fig. 4e and 4f) and neutrophil marker LY6G (Fig. 4g and 4h) were found to be increased in the LPS group and were reduced by **34#** treatment.

34# reduced the level of inflammatory cytokine in the lung tissue of LPS-induced ALI.

The effect of **34#** on inflammatory cytokine expression was evaluated using an ELISA assay. The amount of TNF-α (Fig. 5a and c) and IL-6 (Fig. 5b and d) in serum and BALF were noted to be significantly increased but was markedly reduced following **34#** pretreatment. Furthermore, RT-qPCR was used to evaluate the gene expression of TNF-α, IL-6, IL-1β, ICAM-1, VCAM-1 and MCP-1 (Fig. 5e-j). As expected, LPS-induced gene expression of inflammatory cytokines and adhesion molecules were found to be ameliorated by **34#** treatment. In order to determine how **34#** worked in LPS-induced ALI, the protein level of P-JNK, P-ERK and P-p38 in lung tissue was ascertained by Western blot analysis (Fig. 5k). The results were found to be the same as those in the *in vitro* experiment, where **34#** was found to reduce the phosphorylation of JNK, ERK and P38 in LPS-stimulated lung tissues.

Discussion

MAPKs is a family of serine/threonine protein kinases found in organisms, which includes the JNK, P38, and ERK pathways. They are able to activate the production of a series of stress-related inflammatory mediators[17]. Additionally, the MAPKs/AP-1 signaling pathway regulates the expression of multiple genes, which play a vital role in various pathological processes such as inflammation [18, 19], photoaging[20] and tumors[21]. LPS activates the MAPKs/AP-1 pathway, induces the phosphorylation of JNK, ERK, P38 and further activates AP-1 and c-jun, triggering a series of inflammatory reactions. E Finkin-Groner et al. showed that Indoline-3-propionate can reduce the production of LPS-induced pro-

inflammatory factors by inhibiting the P38 MAPKs/AP-1 pathway[22]. In addition, studies have shown that MAPKs/AP-1 signaling pathways are crucial in O (3)-induced TNF-R-mediated pulmonary toxicity[18], which was also demonstrated by the present experiments. The MAPKs/AP-1 pathway plays an important role in LPS-induced lung injury, and **34#** can inhibit the activation of the MAPKs/AP-1 pathway while serving a protective role. However, our compound was found to have no effect on the NF-κB pathway, which should be further explored.

Inflammatory cell infiltration of lung tissue is an important pathological process of ALI. In ALI, inflammatory cells, such as macrophages, monocytes, and neutrophils, are recruited to the lungs[23]. Intrapulmonary macrophages mainly refer to alveolar macrophages, which are the first line of defense in lung tissue, have functions of phagocytosis and secretion, can synthesize inflammatory factors like tumor necrosis factor, and trigger a cascade of inflammatory responses[24]. The accumulation and infiltration of neutrophils in lung tissue is also a known indication of ALI[25]. The increased expression of vascular endothelial cell adhesion molecules at inflammatory reaction site results in the easy recruitment of inflammatory cells in the lung to the alveoli and lung interstitium, which accumulate in the lungs following their activation [26, 27]. The recruited and activated neutrophils are able to release a large number of metabolites, such as elastase, ROS and arachidonic acid, resulting in the destruction of alveolar walls and capillaries, reduction of the production of alveolar surfactants, and lung cell inflammation and infiltration, which leads to lung tissue damage[28]. Therefore, immunohistochemistry was utilized in order to detect CD68, a marker of monocytes and macrophages, and LY6G, a marker of neutrophils. The corresponding results demonstrated that **34#** can inhibit inflammatory cell infiltration of ALI. In addition, the total cell, monocyte and neutrophil counts in BALF exhibited the inhibitory effect of **34#** on inflammatory cell recruitment.

ALI is also characterized by increased permeability of the alveolar-capillary barrier as well as the presence of a large number of cytokines and pro-inflammatory mediators, which further amplify the inflammatory response of ALI [4]. In the early stages of ALI, alveolar macrophages secrete inflammatory factors and chemokines, such as TNF-α and IL-6 [17]. In the middle stage of ALI, inflammatory factors and chemokines produced by macrophages, platelets, and vascular endothelial cells can chemoattract and recruit granulocytes [22]. In this study, **34#** was found to significantly inhibit the secretion of inflammatory factors in serum and BALF. Meanwhile, the LPS-induced gene expression of adhesion molecules ICAM-1, VCAM-1 and chemokines MCP-1 in the lung was also observed to be inhibited by **34#** administration. Elastase secreted by neutrophils is a serine protease, which can act on the extracellular matrix of endothelial tissue, damage the integrity of the vascular-endothelial barrier, and increase the permeability of the vascular endothelium [23, 29]. The present results showed that **34#** administration significantly reduced protein concentration and total cell counts in BALF after exposure to LPS, which indicate that **34#** may serve as a potential treatment for ALI.

Conclusion

In conclusion, the *in vitro* experiment demonstrated that **34#** can obviously inhibit LPS-induced inflammatory cytokines expression, which may occur through the inhibition of the MAPK/AP-1 pathway. Meanwhile, **34#** treatment was found to attenuate LPS-induced ALI in mice by reducing inflammatory cell infiltration as well as the inflammatory response, indicating that **34#** may serve as a candidate in treating acute lung inflammation and injury.

Declarations

Acknowledgment

We would like to give our sincere gratitude to the reviewers for their constructive comments.

Author Contributions

Data curation, Zaisheng Zhu, Wenjing Jia; Formal analysis, Wenjing Jia; Funding acquisition, Wenting Ding and Zaisheng Zhu; Methodology, Wenjing Jia, Yali Zhang and Xinmiao Chen; Validation, Meihong Wang, Zhengwei Xu and Yelin Tang; Visualization, Bin Zheng and Xinmiao Chen; Writing – original draft, Wenjing Jia; Writing-review & editing, Tao Wei and Zaisheng Zhu.

Funding

This study was supported by the Wenzhou Scientific and Technology Program (Y2020174), and National College Student Innovation and Entrepreneurship Training Program (202010343011), and Wenzhou Medical University Scientific Research Projects of College Students (wyx2020101027).

Data Availability

All data generated or analyzed during this study are included in this published article.

Conflicts of Interest

The authors confirm that there are no conflicts of interest.

References

1. Ware, L. B., and M. A. Matthay. 2000. The acute respiratory distress syndrome. *N Engl J Med* 342 (18): 1334–1349. doi:10.1056/NEJM200005043421806.
2. Bellani, G., J. G. Laffey, T. Pham, E. Fan, L. Brochard, A. Esteban, L. Gattinoni, F. van Haren, A. Larsson, D. F. McAuley, M. Ranieri, G. Rubenfeld, B. T. Thompson, H. Wrigge, A. S. Slutsky, A. Pesenti, L. S. Investigators, and E. T. Group. 2016. Epidemiology, Patterns of Care, and Mortality for Patients With Acute Respiratory Distress Syndrome in Intensive Care Units in 50 Countries. *JAMA* 315 (8): 788–800. doi:10.1001/jama.2016.0291.

3. Diaz, J. V., R. Brower, C. S. Calfee, and M. A. Matthay. 2010. Therapeutic strategies for severe acute lung injury. *Crit Care Med* 38 (8): 1644–1650. doi:10.1097/CCM.0b013e3181e795ee.
4. Matthay, M. A., R. L. Zemans, G. A. Zimmerman, Y. M. Arabi, J. R. Beitler, A. Mercat, M. Herridge, A. G. Randolph, and C. S. Calfee. 2019. Acute respiratory distress syndrome. *Nat Rev Dis Primers* 5 (1): 18. doi:10.1038/s41572-019-0069-0.
5. Zhang, Y., T. Xu, Z. Pan, X. Ge, C. Sun, C. Lu, H. Chen, Z. Xiao, B. Zhang, Y. Dai, and G. Liang. 2018. Shikonin inhibits myeloid differentiation protein 2 to prevent LPS-induced acute lung injury. *Br J Pharmacol* 175 (5): 840–854. doi:10.1111/bph.14129.
6. Manzanares, W., E. Moreira, and G. Hardy. 2021. Pharmaconutrition revisited for critically ill patients with coronavirus disease 2019 (COVID-19): Does selenium have a place? *Nutrition (Burbank, Los Angeles County, Calif.)* 81: 110989. doi:10.1016/j.nut.2020.110989.
7. Xiong, Y., Q. Yin, E. Jin, H. Chen, and S. He, Selenium Attenuates Chronic Heat Stress-Induced Apoptosis via the Inhibition of Endoplasmic Reticulum Stress in Mouse Granulosa Cells. Molecules, 2020, 25, (3), doi:10.3390/molecules25030557.
8. Liu, H. J., Y. Qin, Z. H. Zhao, Y. Zhang, J. H. Yang, D. H. Zhai, F. Cui, C. Luo, M. X. Lu, P. P. Liu, H. W. Xu, K. Li, B. Sun, S. Chen, H. G. Zhou, C. Yang, and T. Sun. 2020. Lentinan-functionalized Selenium Nanoparticles target Tumor Cell Mitochondria via TLR4/TRAF3/MFN1 pathway. *Theranostics* 10 (20): 9083–9099. doi:10.7150/thno.46467.
9. Mita, Y., K. Nakayama, S. Inari, Y. Nishito, Y. Yoshioka, N. Sakai, K. Sotani, T. Nagamura, Y. Kuzuhara, K. Inagaki, M. Iwasaki, H. Misu, M. Ikegawa, T. Takamura, N. Noguchi, and Y. Saito, Selenoprotein P-neutralizing antibodies improve insulin secretion and glucose sensitivity in type 2 diabetes mouse models. *Nature communications*. 2017. 8, (1), 1658, doi: 10.1038/s41467-017-01863-z.
10. Tang, C., S. Li, K. Zhang, J. Li, Y. Han, T. Zhan, Q. Zhao, X. Guo, and J. Zhang. 2020. Selenium deficiency-induced redox imbalance leads to metabolic reprogramming and inflammation in the liver. *Redox Biol* 36: 101519. doi:10.1016/j.redox.2020.101519.
11. Rayman, M. P. Selenium and human health. Lancet, 2012, 379, (9822), 1256–68, doi:10.1016/S0140-6736(11)61452-9.
12. Tindell, R., S. B. Wall, Q. Li, R. Li, K. Dunigan, R. Wood, and T. E. Tipple. 2018. Selenium supplementation of lung epithelial cells enhances nuclear factor E2-related factor 2 (Nrf2) activation following thioredoxin reductase inhibition. *Redox Biol* 19: 331–338. doi:10.1016/j.redox.2018.07.020.
13. Manikova, D., Z. Sestakova, J. Rendekova, D. Vlasakova, P. Lukacova, E. Paegle, P. Arsenyan, and M. Chovanec, Resveratrol-Inspired Benzo[b]selenophenes Act as Anti-Oxidants in Yeast. Molecules, 2018, 23, (2), doi:10.3390/molecules23020507.
14. Chen, W., J. An, J. Guo, Y. Wu, L. Yang, J. Dai, K. Gong, S. Miao, S. Xi, and J. Du. 2018. Sodium selenite attenuates lung adenocarcinoma progression by repressing SOX2-mediated stemness. *Cancer Chemother Pharmacol* 81 (5): 885–895. doi:10.1007/s00280-018-3561-4.

15. Spengler, G., M. Gajdacs, M. A. Marc, E. Dominguez-Alvarez, and C. Sanmartin, Organoselenium Compounds as Novel Adjuvants of Chemotherapy Drugs-A Promising Approach to Fight Cancer Drug Resistance. Molecules, 2019, 24, (2), doi:10.3390/molecules24020336.
16. Hariharan, S., and S. Dharmaraj. 2020. Selenium and selenoproteins: it's role in regulation of inflammation. *Inflammopharmacology* 28 (3): 667–695. doi:10.1007/s10787-020-00690-x.
17. Kim, E. K., and E. J. Choi. 2010. Pathological roles of MAPK signaling pathways in human diseases. *Biochim Biophys Acta* 1802 (4): 396–405. doi:10.1016/j.bbadis.2009.12.009.
18. Cho, H. Y., D. L. Morgan, A. K. Bauer, and S. R. Kleeberger. 2007. Signal transduction pathways of tumor necrosis factor–mediated lung injury induced by ozone in mice. *Am J Respir Crit Care Med* 175 (8): 829–839. doi:10.1164/rccm.200509-1527OC.
19. Limtrakul, P., S. Yodkeeree, P. Pitchakarn, and W. Punfa. 2016. Anti-inflammatory effects of proanthocyanidin-rich red rice extract via suppression of MAPK, AP-1 and NF-kappaB pathways in Raw 264.7 macrophages. *Nutr Res Pract* 10 (3): 251–258. doi:10.4162/nrp.2016.10.3.251.
20. Chaiprasongsuk, A., J. Lohakul, K. Soontrapa, S. Sampattavanich, P. Akarasereenont, and U. Panich. 2017. Activation of Nrf2 Reduces UVA-Mediated MMP-1 Upregulation via MAPK/AP-1 Signaling Cascades: The Photoprotective Effects of Sulforaphane and Hispidulin. *J Pharmacol Exp Ther* 360 (3): 388–398. doi:10.1124/jpet.116.238048.
21. Zhao, L., T. Zhang, H. Geng, Z. Q. Liu, Z. F. Liang, Z. Q. Zhang, J. Min, D. X. Yu, and C. Y. Zhong. 2018. MAPK/AP-1 pathway regulates benzidine-induced cell proliferation through the control of cell cycle in human normal bladder epithelial cells. *Oncol Lett* 16 (4): 4628–4634. doi:10.3892/ol.2018.9155.
22. Finkin-Groner, E., D. Moradov, H. Shifrin, C. Bejar, A. Nudelman, and M. Weinstock. 2015. Indoline-3-propionate and 3-aminopropyl carbamates reduce lung injury and pro-inflammatory cytokines induced in mice by LPS. *Br J Pharmacol* 172 (4): 1101–1113. doi:10.1111/bph.12982.
23. Villar, J., J. Blanco, and R. M. Kacmarek. 2016. Current incidence and outcome of the acute respiratory distress syndrome. *Curr Opin Crit Care* 22 (1): 1–6. doi:10.1097/MCC.0000000000000266.
24. Beck-Schimmer, B., R. Schwendener, T. Pasch, L. Reyes, C. Booy, and R. C. Schimmer. 2005. Alveolar macrophages regulate neutrophil recruitment in endotoxin-induced lung injury. *Respir Res* 6: 61. doi:10.1186/1465-9921-6-61.
25. Wessels, I., J. T. Pupke, K. T. von Trotha, A. Gombert, A. Himmelsbach, H. J. Fischer, M. J. Jacobs, L. Rink, and J. Grommes. 2020. Zinc supplementation ameliorates lung injury by reducing neutrophil recruitment and activity. *Thorax* 75 (3): 253–261. doi:10.1136/thoraxjnl-2019-213357.
26. Kawashima, M., M. Kuwamura, M. Takeya, and J. Yamate. 2004. Morphologic characteristics of pulmonary macrophages in cetaceans: particular reference to pulmonary intravascular macrophages as a newly identified type. *Vet Pathol* 41 (6): 682–686. doi:10.1354/vp.41-6-682.
27. Belperio, J. A., M. P. Keane, M. D. Burdick, V. Londhe, Y. Y. Xue, K. Li, R. J. Phillips, and R. M. Strieter. 2002. Critical role for CXCR2 and CXCR2 ligands during the pathogenesis of ventilator-induced lung injury. *J Clin Invest* 110 (11): 1703–1716. doi:10.1172/JCI15849.

28. Williams, A. E., and R. C. Chambers. 2014. The mercurial nature of neutrophils: still an enigma in ARDS? *Am J Physiol Lung Cell Mol Physiol* 306 (3): L217–L230. doi:10.1152/ajplung.00311.2013.
29. Chalmers, J. D., C. S. Haworth, M. L. Metersky, M. R. Loebinger, F. Blasi, O. Sibila, A. E. O'Donnell, E. J. Sullivan, K. C. Mange, C. Fernandez, J. Zou, C. L. Daley, and W. Investigators. 2020. Phase 2 Trial of the DPP-1 Inhibitor Brensocatib in Bronchiectasis. *N Engl J Med* 383 (22): 2127–2137. doi:10.1056/NEJMoa2021713.

Table

Table 1. Primer sequences used in this study.

Gene	Species	Forward primer	Reverse primer
TNF-α	mouse	CAGGGGCCACCACGCTCTTC	TTTGTGAGTGTGAGGGTCTGG
IL-6	mouse	GAGGATACCACTCCCAACAGACC	AAGTGCATCATCGTTGTTCATACA
IL-1β	mouse	ACTCCTTAGTCCTCGGCCA	CCATCAGAGGCAAGGAGGAA
VCAM-1	mouse	TGCCGAGCTAAATTACACATTG	CCTTGTGGAGGGATGTACAGA
ICAM-1	mouse	GCCTTGGTAGAGGTGACTGAG	GACCGGAGCTGAAAAGTTGTA
MCP-1	mouse	TCACCTGCTGCTACTCATTCACCA	TACAGCTTCTTTGGGACACCTGCT
β-actin	mouse	CCGTGAAAAGATGACCCAGA	TACGACCAGAGGCATACAG

Figures

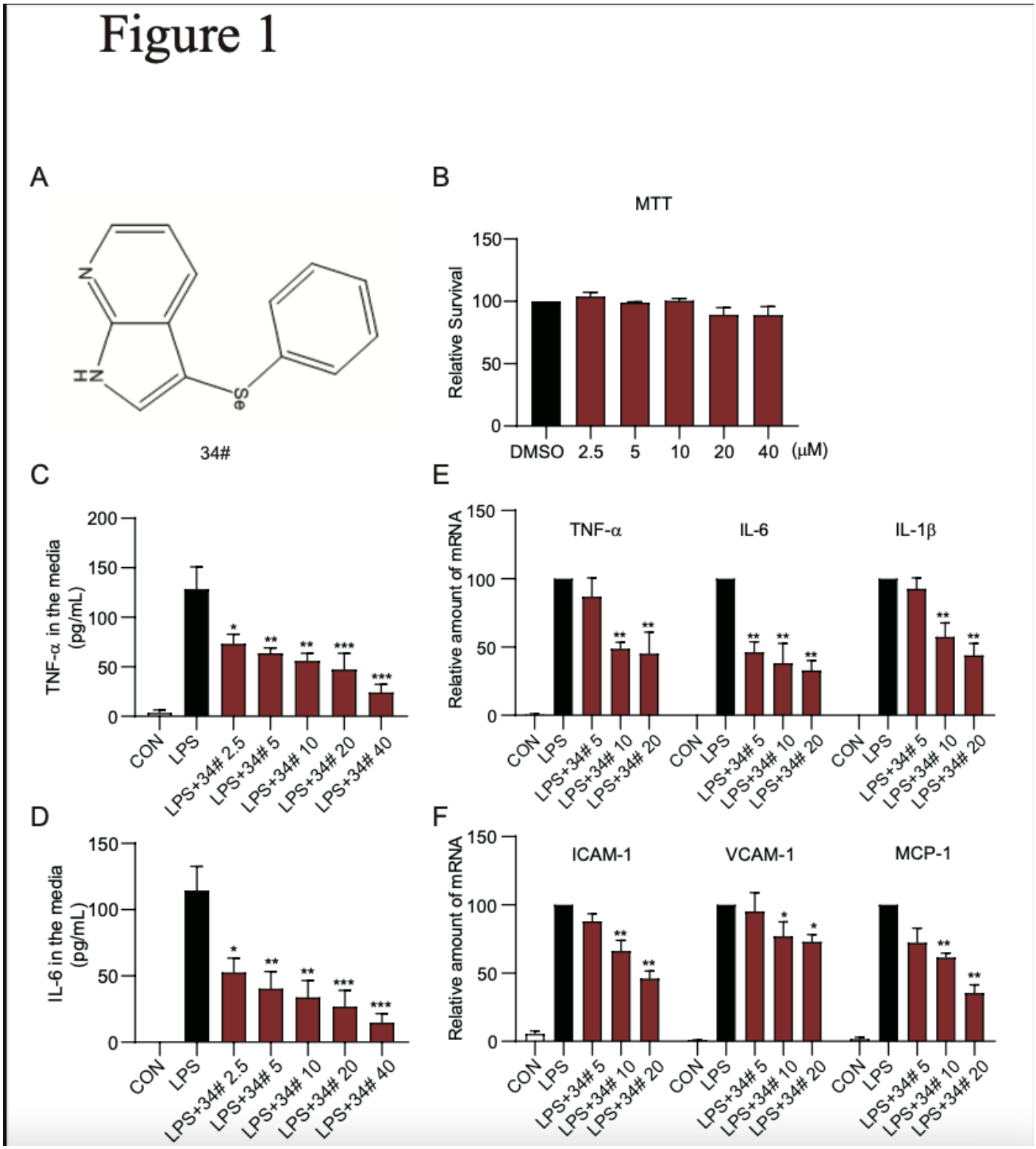

Figure 1

Effect of Compounds 34# on cytokines release in LPS-stimulated macrophages. (a) The chemical structure of 34#. (b) Macrophages were pretreated with various concentrations of 34# for 24 h, and cell viability was analyzed via MTT assay. (c-d) Macrophages were plated at a density of 5 x 105/plate and were cultured overnight in medium containing 10% serum, which was pretreated with 34# at 2.5, 5, 10, 20 or 40 μM for 30 min followed by stimulation with 0.5 μg/mL LPS for 24 h. DMSO was used as the vehicle

control. Supernatants were collected and analyzed for TNF-α (C) and IL-6 (D) release using ELISA. (e-f) MPMs were pretreated with the vehicle control (DMSO) and 34# (5, 10 or 20 μM) for 30 min, after which they were incubated with LPS at 0.5 μg/mL for 6 h. The mRNA levels of TNF-α, IL-6, IL-1β VCAM-1, ICAM-1 and MCP-1 were quantified by RT-qPCR. Data were normalized to β-actin and were expressed as % of LPS group. Data were normalized to total protein concentration from the same plate and were expressed as fold change relative to LPS group. (*P < 0.05, **P < 0.01, ***P < 0.001 vs LPS group).

Figure 2

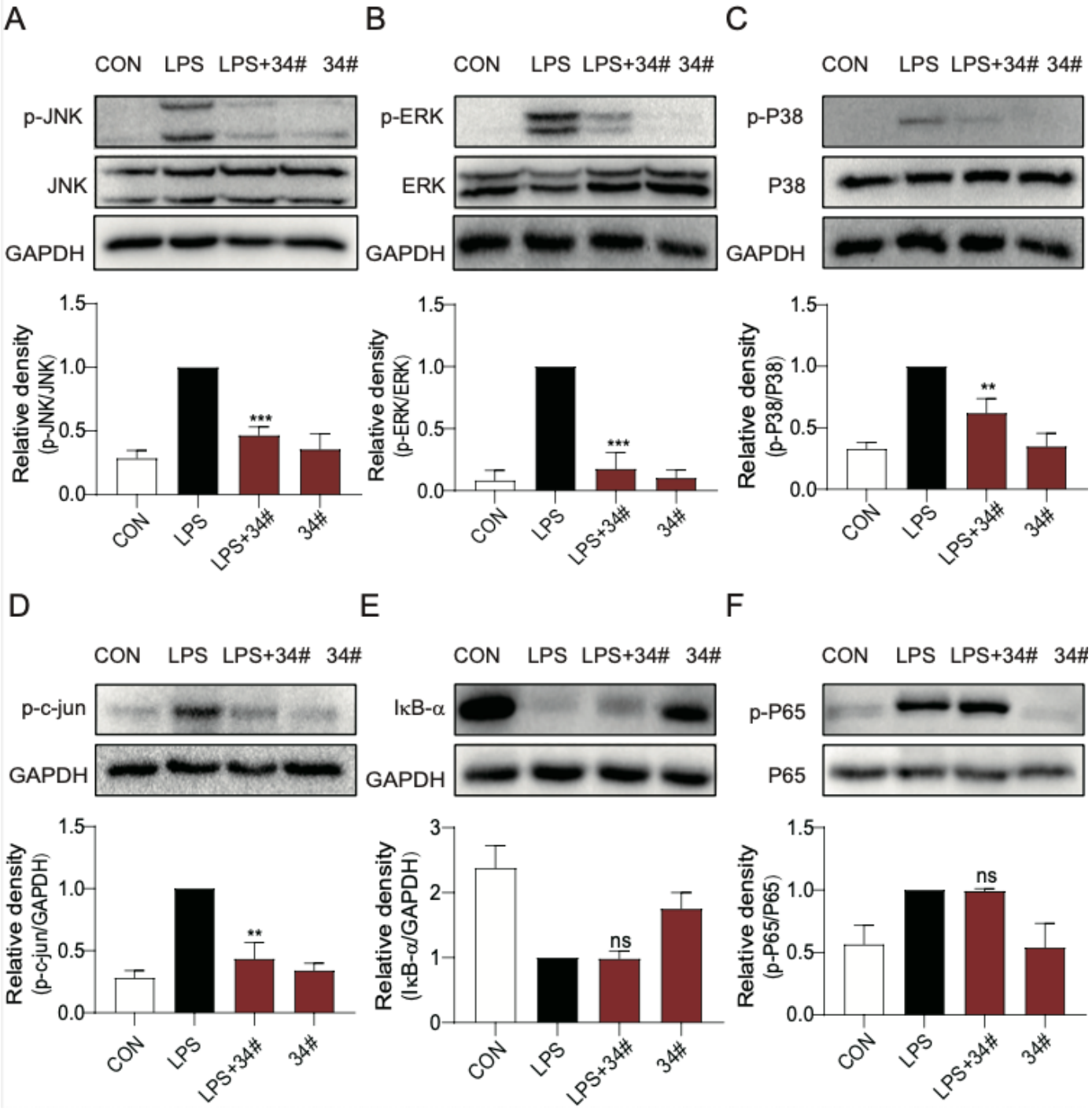

Figure 2

Effect of 34# on LPS-induced MAPK phosphorylation and NF-κB activation in macrophages. MPMs were pretreated with 34# at 10 μM for 30 min followed by incubation with LPS (0.5 μg/mL) for 15 min. The protein levels of p-JNK (a), p-ERK (b), p-P38 (c) and IκB-α (e) were measured by western blot. Total protein of JNK, ERK, P38 and GAPDH were used as loading control. Protein levels of p-c-jun (d) and p-P65 (f) were examined by Western blot. MPMs were pretreated with 34# at 10 μM for 30 min followed by stimulation with LPS (0.5 μg/mL) for 30 min. Each bar represents mean ± SEM of independent experiments. (**P < 0.01, ***P < 0.001 compared with LPS group).

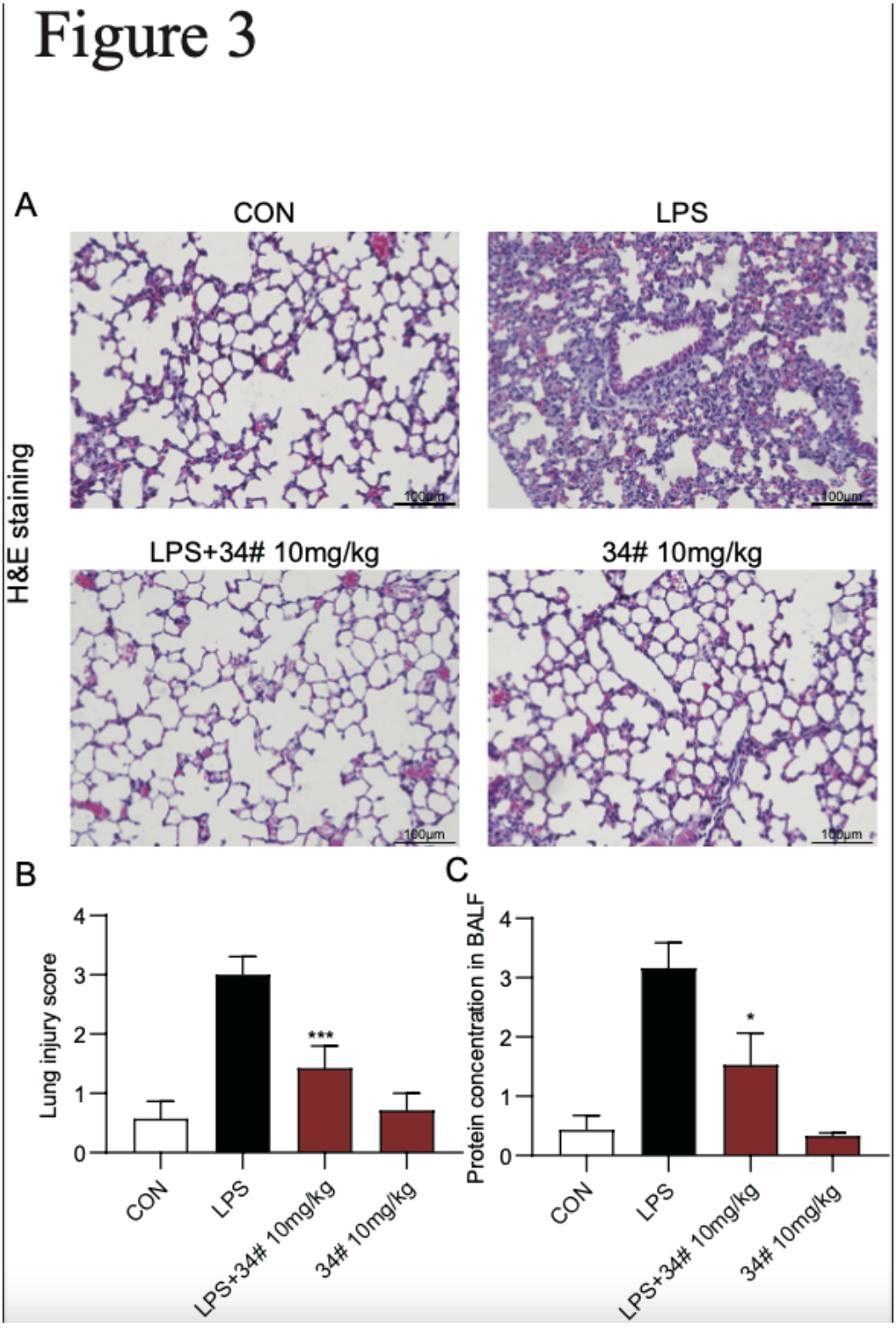

Figure 3

34# diminishes the severity of LPS-induced acute lung injury in mice. (a) Representative images demonstrate H&E staining of lung sections from control (saline) and mice subjected to LPS. Mice received 34# (10 mg/kg, i.g.) once a day for 3 consecutive days followed by intracheal injection of 5 mg/kg LPS, and lungs were sampled 6 h later for analysis (Scale bars: 100 μm). (b) Lung injury score as assessed by histological analysis of lung tissues. (c) Protein concentration in BALF. Data are shown as mean ± SEM (n ≥ 5, (*P < 0.05, ***P < 0.001 compared with LPS group).

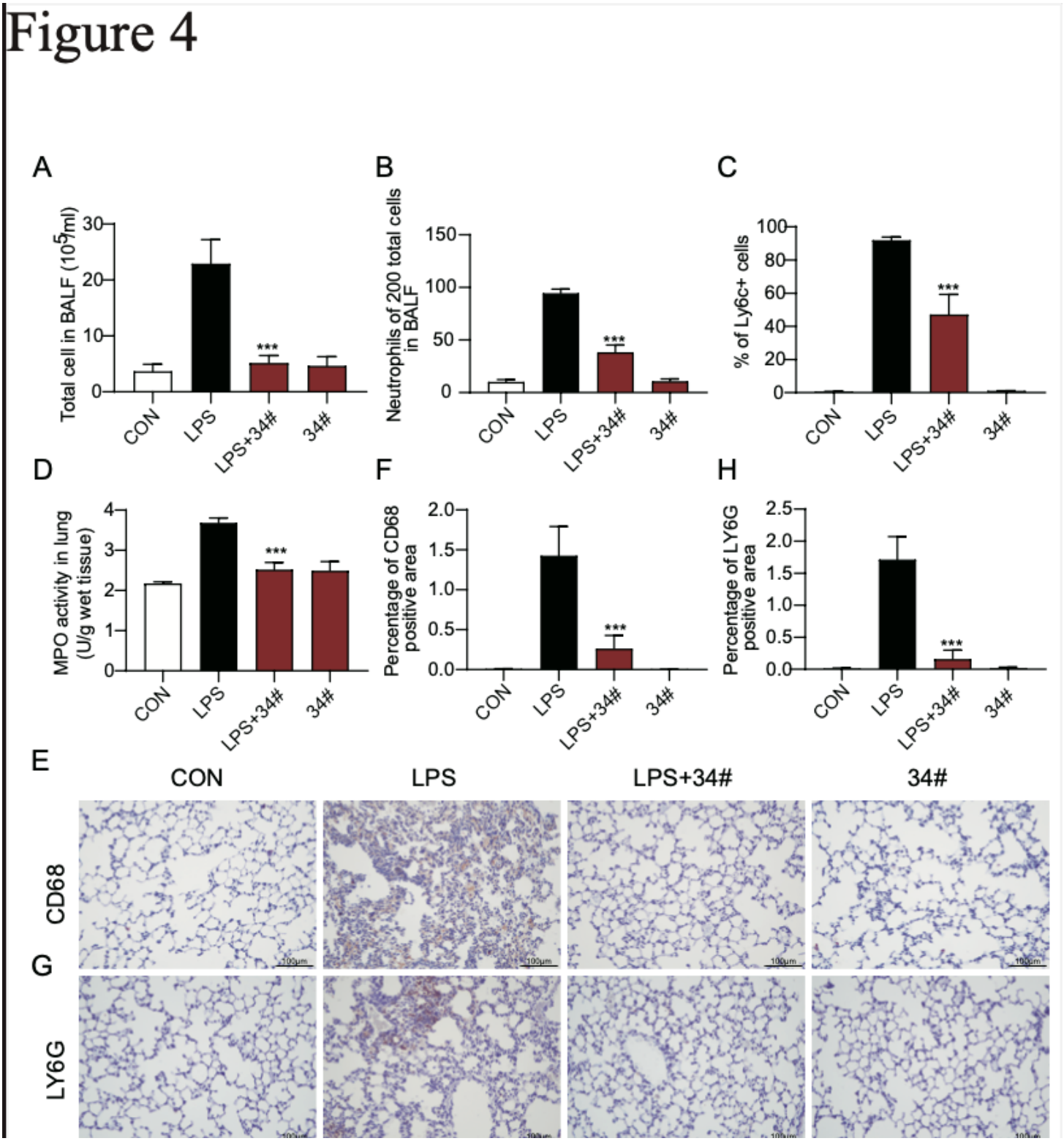

Figure 4

34# reduced LPS-induced inflammatory cell infiltration in lung tissue of ALI mice. C57BL/6 mice were pretreated with 10 mg/kg 34# via oral administration 3 days prior to LPS exposure. (a) Total Cell counts in BALF. (b) Neutrophils and (c) Monocyte in BALF. (d) MPO activity in lung tissue. (e) Immunohistochemical staining for macrophage marker CD68 in lung tissues of mice challenged with LPS. Immunoreactivity is shown in brown (scale bar = 100 μm). (f) Quantification of positive lung tissue staining for CD68. (g) Representative image of immunohistochemistry of neutrophils in lung tissues detected with murine neutrophil marker protein LY6G. (h) Quantification of positive lung tissues staining for LY6G. Data are shown as mean ± SEM (n ≥ 5, (***P < 0.001 compared with LPS group).

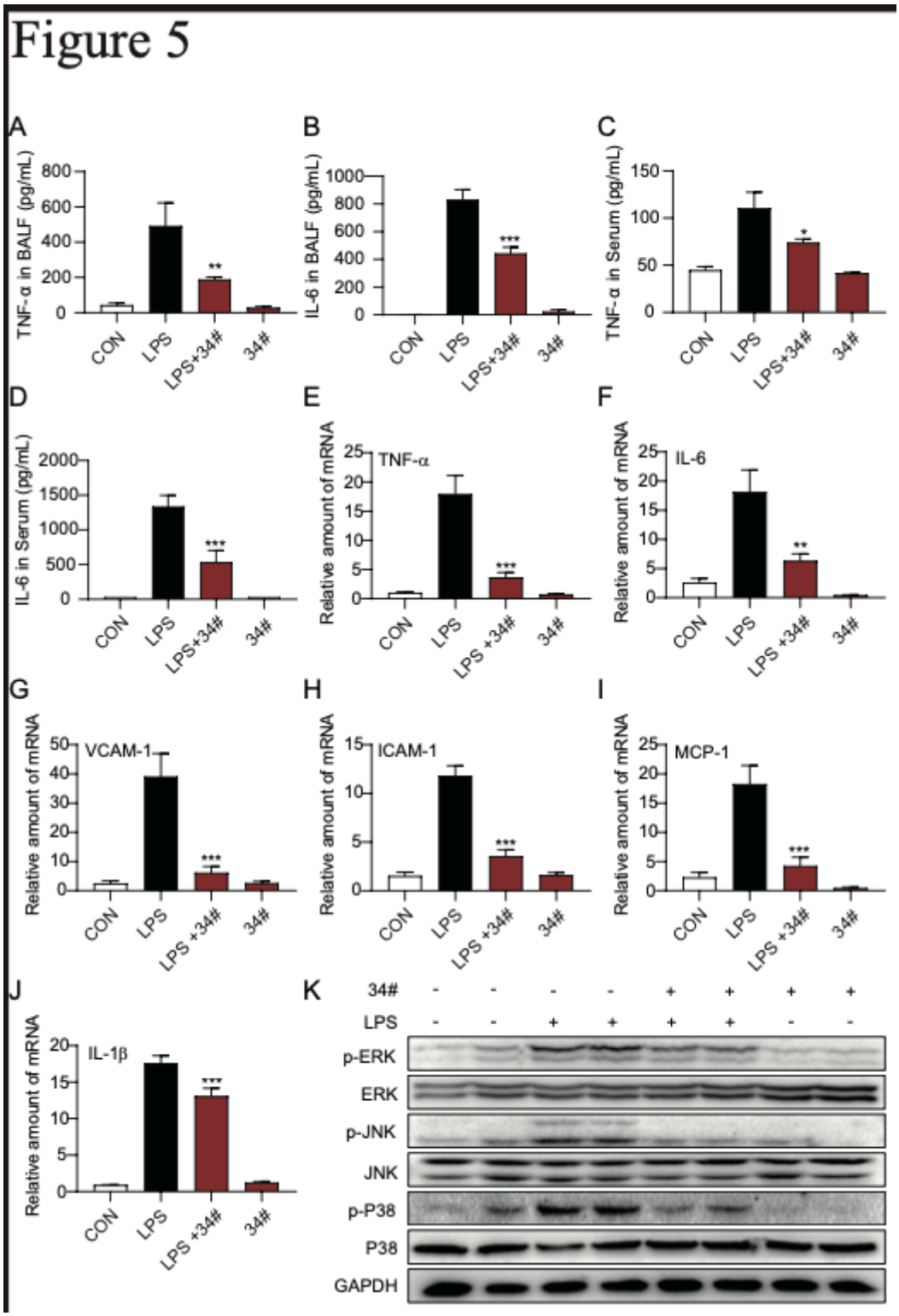

Figure 5

34# reduced the level of inflammatory cytokine in the lung tissue of LPS-induced ALI. ELISA detection of (a, c) TNF-α and (b, d) IL-6 in BALF and serum from the experimental mice was carried out. (e-j) The mRNA levels of inflammatory cytokines and adhesion molecule in lung tissues were determined by RT-qPCR after LPS treatment. Cytokine expression was normalized to β-actin. (k) The protein level of p-JNK,

p-ERK and p-P38 in lung tissue was ascertained by Western blot analysis. Each bar represents mean ± SEM of independent experiments. (*P < 0.05, **P < 0.01, ***P < 0.001 compared with LPS group).